

Cooperative Visual Convex Area Coverage using a Tessellation-free Strategy*

Sotiris Papatheodorou¹ and Anthony Tzes¹

Abstract—The objective in this article is to develop a control strategy for coverage purposes of a convex region by a fleet of Mobile Aerial Agents (MAAs). Each MAA is equipped with a downward facing camera that senses a convex portion of the area while its altitude flight is constrained. Rather than relying on typical Voronoi-like tessellations of the area to be covered, a scheme focusing on the assignment to each MAA of certain parts of the mosaic of the current covered area is proposed. A gradient ascent algorithm is then employed to increase in a monotonic manner the covered area by the MAA-fleet. Simulation studies are offered to illustrate the effectiveness of the proposed scheme.

Index Terms—Cooperative Control, Autonomous Systems, Area Coverage, Robotic Camera Networks

I. INTRODUCTION

Area coverage over a planar region by ground agents has been studied extensively when the sensing patterns of the agents are circular [1], [2]. The majority of these techniques is based on a Voronoi or similar partitioning [3], [4], [5] of the region of interest and the employed control techniques include distributed optimization, model predictive control [6] and game theory [7] among others. There has also been significant work concerning arbitrary sensing patterns [8], [9], [10] while avoiding the usage of Voronoi partitioning [11], [12]. Convex as well as non-convex regions of interest have been studied [13], [14].

A multitude of algorithms has been developed for mapping by MAAs [15], [16], [17], [18] relying mostly in Voronoi-based tessellations of the region or path planning. Extensive research has been conducted in the field of area monitoring by MAAs equipped with cameras [19], [20]. In these pioneering research efforts, no constraints are imposed on the altitude of the MAAs and overlapping between their covered regions is considered advantageous compared to the same region sensed by a single MAA. There is also work on ground target detection and tracking [21] by a team of MAAs as well as the connectivity and energy consumption of MAA networks [22], [23].

This article examines the persistent coverage problem of a convex planar region by a network of MAAs. The MAAs are assumed to have downwards facing visual sensors with arbitrary convex sensing footprints. Thus, both the covered

area and the coverage quality of that area are dependent on the altitude of each MAA. MAAs at higher altitudes cover more area but with a lower coverage quality compared to MAAs at lower altitudes. A partitioning scheme of the sensed region, similar to [11], is employed in order to derive a gradient-based distributed control law. This control law leads the network to a locally optimal configuration with respect to a combined coverage-quality criterion. This work is an extension of [24] from circular sensing footprints to any convex sensing footprint. Algorithmic implementations of the proposed control scheme are provided as free and open-source (Matlab-based) code in an online repository.

The problem statement and the optimization criterion are formulated in Section II. The coverage quality function and its properties are presented in Section III while the sensed space partitioning scheme is defined in Section IV. The distributed control law is derived in Section V. Simulation studies highlighting the efficiency of the proposed control law in comparison to other control schemes are provided in Section VI followed by concluding remarks.

II. PROBLEM STATEMENT

We assume a compact and convex region $\Omega \subset \mathbb{R}^2$ which is under surveillance. We also assume a team of n MAAs, each positioned at $X_i = [x_i \ y_i \ z_i]^T$, $i \in I_n$ and having an orientation θ_i , $i \in I_n$ with respect to the yaw axis, where $I_n = \{1, \dots, n\}$. In addition, we define the vector $q_i = [x_i \ y_i]^T$, $q_i \in \Omega$, denoting the projection of each MAA on the ground. Each MAA can fly between two predefined minimum and maximum altitudes z_i^{\min} and z_i^{\max} respectively, with $z_i^{\min} < z_i^{\max}$, thus $z_i \in [z_i^{\min}, z_i^{\max}]$, $i \in I_n$. It is assumed that $z_i^{\min} > 0$, $\forall i \in I_n$, since setting the minimum altitude to zero could potentially lead to some MAAs crashing on the ground. The minimum altitude z_i^{\min} ensures that the MAAs will fly above ground obstacles, whereas the maximum altitude z_i^{\max} that they will remain within range of their base station.

Instead of using a complete dynamic model, such as the quadrotor helicopter dynamics in [25], a simplified single integrator dynamic model is used. The MAAs are approximated by point masses, thus each one's kinodynamic model is

$$\begin{aligned} \dot{q}_i &= u_{i,q}, & q_i &\in \Omega, & u_{i,q} &\in \mathbb{R}^2, \\ \dot{z}_i &= u_{i,z}, & z_i &\in [z_i^{\min}, z_i^{\max}], & u_{i,z} &\in \mathbb{R}, \\ \dot{\theta}_i &= \omega_i, & \theta_i &\in \mathbb{R}, & \omega_i &\in \mathbb{R}. \end{aligned} \quad (1)$$

where $[u_{i,q}^T, u_{i,z}, \omega_i]^T$ is the corresponding control input for each MAA (node). In the sequel, all MAAs are assumed to

*This work has received funding from the European Union's Horizon 2020 Research and Innovation Programme under the Grant Agreement No.644128, AEROWORKS.

¹ The authors are with New York University Abu Dhabi, United Arab Emirates; This work was partially completed while the authors were with University of Patras, Greece. Corresponding author's email: anthony.tzes@nyu.edu

have common minimum z^{\min} and maximum z^{\max} altitudes, although the results produced could be generalized to account for different altitude constraints among MAAs.

Regarding the sensing performance of the MAAs, they are assumed to be equipped with identical, downwards facing visual sensors. Each sensor is able to cover a convex region on the ground. As the altitude of an MAA increases, the area of the region it surveys also increases, as shown in Figure 1. Without loss of generality, we define a base sensing pattern C^b as the region surveyed by an MAA positioned at $X_i = [0 \ 0 \ z^{\min}]^T$ with an orientation $\theta_i = 0$. We assume that there exists a parametrization $\gamma(k)$ of the boundary ∂C^b of this base sensing pattern

$$\partial C^b = \{q \in \mathbb{R}^2 : q = \gamma(k), k \in K\} \quad (2)$$

where the interval K is dependent on the parametrization and

$$\gamma(k) = \begin{bmatrix} \gamma_x(k) \\ \gamma_y(k) \end{bmatrix}, k \in K$$

Thus the sensing pattern of an MAA located at $X_i = [x_i \ y_i \ z_i]^T$ with an orientation θ_i can be derived by scaling according to its altitude, rotating around the origin, and finally translating the base sensing pattern as follows

$$C_i(X_i, \theta_i) = q_i + \mathbf{R}(\theta_i) \frac{z_i}{z^{\min}} C^b \quad (3)$$

where $\mathbf{R}(\cdot)$ is the 2×2 rotation matrix. Additionally, we define the minimum base sensing pattern radius as

$$r_b^{\min} = \min \{\|q\|, \forall q \in \partial C^b\}.$$

This radius is constant since the base sensing pattern is independent of the agents' states.

As the altitude of an MAA increases, the visual coverage quality of its sensed region decreases. We define a coverage quality function $f(z_i) : [z^{\min}, z^{\max}] \rightarrow [0, 1]$ which is dependent on the MAA's altitude constraints z^{\min} and z^{\max} . This coverage quality is assumed to be uniform throughout the sensed region C_i . The greater the value of $f(z_i)$, the better the coverage quality of C_i . The exact definition and properties of this coverage quality function are presented in Section III.

Each point $q \in \Omega$ is assigned an importance weight through a space density function $\phi : \Omega \rightarrow \mathbb{R}^+$, which expresses the a priori information regarding the region of interest.

Finally, we define the joint coverage-quality objective function

$$\mathcal{H} \triangleq \int_{\Omega} \max_{i \in I_n} f(z_i) \phi(q) dq. \quad (4)$$

III. COVERAGE QUALITY FUNCTION

A uniform coverage quality throughout each sensed region C_i can be used to effectively model downward facing cameras [26], [27] that provide uniform quality throughout the whole image. The uniform coverage quality function $f(z_i) : [z^{\min}, z^{\max}] \rightarrow [0, 1]$ was chosen to be

$$f(z_i) = \begin{cases} \frac{\left((z_i - z^{\min})^2 - (z^{\max} - z^{\min})^2 \right)^2}{(z^{\max} - z^{\min})^4}, & q \in C_i \\ 0, & q \notin C_i \end{cases} \quad (5)$$

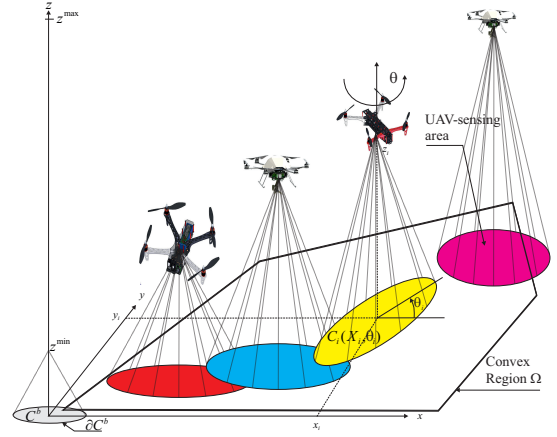


Fig. 1. MAA-visual area coverage concept

A plot of this function can be seen in Figure 2 [Left]. This function was chosen so that $f(z^{\min}) = 1$, $f(z^{\max}) = 0$ and because $f(z_i)$ is first order differentiable with respect to z_i , or $\frac{\partial f(z_i)}{\partial z_i}$ exists within C_i , which is a property that will be required when deriving the control law in Section V.

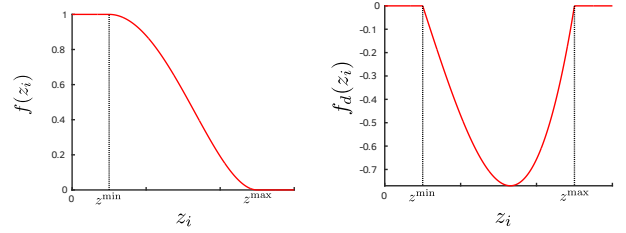


Fig. 2. Uniform coverage quality function [Left] and its derivative [Right].

The derivative $f_d(z_i) \triangleq \frac{\partial f(z_i)}{\partial z_i} : [z^{\min}, z^{\max}] \rightarrow [f_d^{\min}, 0]$ is evaluated as

$$f_d(z_i) = \begin{cases} \frac{4(z_i - z^{\min}) \left[(z_i - z^{\min})^2 - (z^{\max} - z^{\min})^2 \right]}{(z^{\max} - z^{\min})^4}, & q \in C_i \\ 0, & q \notin C_i \end{cases} \quad (6)$$

where $f_d^{\min} = f_d \left(z^{\min} + \frac{\sqrt{3}}{3} (z^{\max} - z^{\min}) \right) = -\frac{8\sqrt{3}}{9(z^{\max} - z^{\min})}$. A plot of this function can be seen in Figure 2 [Right].

IV. SENSED SPACE PARTITIONING

The assignment of responsibility regions to the nodes is achieved in a manner similar to [11], where only the subset of Ω sensed by the nodes is partitioned. Each node is assigned a cell

$$W_i \triangleq \{q \in \Omega : f(z_i) > f(z_j), j \neq i\}, i \in I_n. \quad (7)$$

These cells do not comprise a complete tessellation of the sensed region because they do not include regions that are sensed by multiple nodes with the same coverage quality. We define the set

$$I^l = \{i, j \in I_n, i \neq j : C_i \cap C_j \neq \emptyset \wedge f(z_i) = f(z_j) = f^l\}$$

which contains all the nodes with overlapping sensed regions and common coverage quality f^l . In general, there can be multiple such regions, each with a different coverage quality. We denote the number of such regions L . These regions are not assigned to any node and are defined as

$$W_c^l \triangleq \left\{ \exists i, j \in I^l, i \neq j: q \in C_i \cap C_j \right\}, l \in I_L. \quad (8)$$

Because the coverage quality is uniform, $\partial W_j \cap \partial W_i$ is either an arc of ∂C_i if $f(z_i) > f(z_j)$ or an arc of ∂C_j if $f(z_i) < f(z_j)$. If the sensing region of a node i is contained within the sensing region of another node j , i.e. $C_i \cap C_j = C_i$, then $W_i = C_i$ and $W_j = C_j \setminus C_i$. An example partitioning with all of the aforementioned cases illustrated can be seen in Figure 3 [Left], where the boundaries of the sensing regions ∂C_i are in dashed red and the boundaries of the cells ∂W_i in solid black. Nodes 1 and 2 are at the same altitude so their common covered region W_c^1 shown in gray is left unassigned. The sensing region of node 3 contains the sensing region of node 4 and nodes 5, 6 and 7 illustrate the general case.

By utilizing this partitioning scheme, the network's coverage performance can be written as

$$\mathcal{H} = \sum_{i \in I_n} \int_{W_i} f(z_i) \phi(q) dq + \sum_{l=1}^L \int_{W_c^l} f^l \phi(q) dq. \quad (9)$$

Definition 1: We define the neighbors N_i of node i as

$$N_i \triangleq \{j \neq i: C_j \cap C_i \neq \emptyset\}. \quad (10)$$

The neighbors of node i are those nodes that sense at least a part of the region that node i senses. It is clear that, due to the partitioning scheme used, only the nodes in N_i need to be considered when creating W_i .

Remark 1: The aforementioned partitioning is a complete tessellation of the sensed region $\bigcup_{i \in I_n} C_i$. However it is not a complete tessellation of Ω . The neutral region not assigned by the partitioning scheme is denoted as $\mathcal{O} = \Omega \setminus \left(\bigcup_{i \in I_n} W_i \cup \bigcup_{l=1}^L W_c^l \right)$.

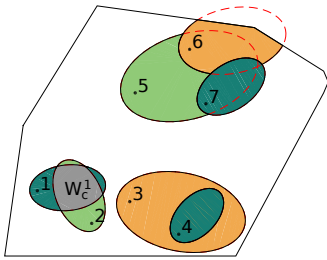


Fig. 3. Sensed space partitioning examples.

V. SPATIALLY DISTRIBUTED COORDINATION ALGORITHM

Based on the nodes kinodynamics (1), their sensing performance (3) and the coverage criterion (9), a gradient based control law is designed. The control law utilizes the

partitioning scheme (7) and results in monotonic increase of the joint coverage–quality criterion \mathcal{H} .

Theorem 1: In an MAA visual network consisting of nodes governed by the kinematics in (1), sensing performance as in (3) and using the space partitioning (7), the control law

$$u_{i,q} = \alpha_{i,q} \left[\int_{\partial W_i \cap \partial \mathcal{O}} v_i^j n_i f(z_i) \phi(q) dq + \sum_{j \in N_i} \int_{\partial W_i \cap \partial W_j} v_i^j n_i (f(z_i) - f(z_j)) \phi(q) dq \right] \quad (11)$$

$$u_{i,z} = \alpha_{i,z} \left[\int_{W_i} f^d(z_i) \phi(q) dq + \int_{\partial W_i \cap \partial \mathcal{O}} v_i^j \cdot n_i f(z_i) \phi(q) dq + \sum_{j \in N_i} \int_{\partial W_i \cap \partial W_j} v_i^j \cdot n_i (f(z_i) - f(z_j)) \phi(q) dq \right] \quad (12)$$

$$\omega_i = \alpha_{i,\theta} \left[\int_{\partial W_i \cap \partial \mathcal{O}} \tau_i^j \cdot n_i f(z_i) \phi(q) dq + \sum_{j \in N_i} \int_{\partial W_i \cap \partial W_j} \tau_i^j \cdot n_i (f(z_i) - f(z_j)) \phi(q) dq \right] \quad (13)$$

where $\alpha_{i,q}$, $\alpha_{i,z}$, $\alpha_{i,\theta}$ are positive constants, v_i^j , v_i^i and τ_i^j are the Jacobian matrices of the points $q \in \partial W_i$ with respect to q_i , z_i and θ_i as defined in equations (14), (16) and (17) respectively and n_i the outward pointing normal vector of W_i , maximizes the performance criterion (9) monotonically along the nodes' trajectories, leading in a locally optimal configuration.

Proof: We are interested in a gradient–based control law in the form

$$u_{i,q} = \alpha_{i,q} \frac{\partial \mathcal{H}}{\partial q_i}, \quad u_{i,z} = \alpha_{i,z} \frac{\partial \mathcal{H}}{\partial z_i}, \quad \omega_i = \alpha_{i,\theta} \frac{\partial \mathcal{H}}{\partial \theta_i}$$

in order to guarantee monotonic increase of the optimization criterion \mathcal{H} .

We will begin by evaluating $\frac{\partial \mathcal{H}}{\partial q_i}$. Through usage of the Leibniz integral rule, the neighbor definition in 10 and since $\frac{\partial f(z_i)}{\partial q_i} = \frac{\partial f(z_j)}{\partial q_i} = 0$, we obtain

$$\frac{\partial \mathcal{H}}{\partial q_i} = \int_{W_i} v_i^j n_i f(z_i) \phi(q) dq + \sum_{j \in N_i} \int_{\partial W_i \cap \partial W_j} v_j^i n_j f(z_j) \phi(q) dq$$

where v_j^i stands for the Jacobian matrix with respect to q_i of the points $q \in \partial W_j$,

$$v_j^i(q) \triangleq \frac{\partial q}{\partial q_i}, \quad q \in \partial W_j, \quad i, j \in I_n \quad (14)$$

and n_i for the outwards unit normal vector on ∂W_i .

The boundary ∂W_i can be decomposed into disjoint sets as

$$\partial W_i = \{\partial W_i \cap \partial \Omega\} \cup \{\partial W_i \cap \partial \mathcal{O}\} \cup \left\{ \bigcup_{j \neq i} (\partial W_i \cap \partial W_j) \right\} \cup \left\{ \bigcup_{l=1}^L (\partial W_i \cap \partial W_c^l) \right\}. \quad (15)$$

These sets represent the parts of ∂W_i that lie on the boundary of Ω , the boundary of the node's sensing region, the parts that are common between the boundary of the cell of node i and those of other nodes and finally the parts that lie on the boundary of some unassigned region covered by multiple nodes. This decomposition can be seen in Figure 4 with the sets $\partial W_i \cap \partial \Omega$, $\partial W_i \cap \partial \mathcal{O}$, $\bigcup_{j \neq i} (\partial W_i \cap \partial W_j)$ and $\bigcup_{l=1}^L (\partial W_i \cap \partial W_c^l)$ appearing in solid purple, red, green and blue respectively.

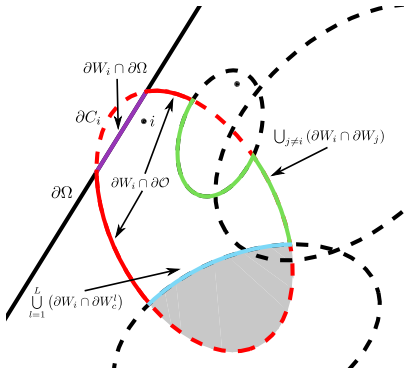


Fig. 4. Decomposition of ∂W_i into disjoint sets.

At $q \in \partial \Omega$ it holds that $v_i^i = \mathbf{0}_{2 \times 2}$ since we assume the region of interest is static. In addition, at $q \in \partial W_i \cap \partial W_c^l$ it holds that $v_i^i = \mathbf{0}_{2 \times 2}$ since $\partial W_i \cap \partial W_c^l$ are arcs of some sensed region ∂C_j and thus independent of the state of node i . Combining this with the boundary decomposition (15) we obtain

$$\begin{aligned} \frac{\partial \mathcal{H}}{\partial q_i} &= \int_{\partial W_i \cap \partial \mathcal{O}} v_i^i n_i f(z_i) \phi(q) dq \\ &+ \sum_{j \in \mathcal{N}_i} \int_{\partial W_i \cap \partial W_j} v_i^i n_i f(z_i) \phi(q) dq \\ &+ \sum_{j \in \mathcal{N}_i} \int_{\partial W_j \cap \partial W_i} v_j^i n_j f(z_j) \phi(q) dq. \end{aligned}$$

Because the boundary $\partial W_i \cap \partial W_j$ is common among nodes i and j , it holds that $v_j^i = v_i^i$ when evaluated over it and that $n_j = -n_i$. Finally, the sums and the integrals within them can be combined and the final form of the planar control law is produced

$$\begin{aligned} \frac{\partial \mathcal{H}}{\partial q_i} &= \int_{\partial W_i \cap \partial \mathcal{O}} v_i^i n_i f(z_i) \phi(q) dq + \\ &\sum_{j \in \mathcal{N}_i} \int_{\partial W_i \cap \partial W_j} v_i^i n_i (f(z_i) - f(z_j)) \phi(q) dq. \end{aligned}$$

By following a similar procedure, defining

$$v_j^i(q) \triangleq \frac{\partial q}{\partial z_i}, \quad q \in \partial W_j, \quad i, j \in I_n \quad (16)$$

and

$$\tau_j^i(q) \triangleq \frac{\partial q}{\partial \theta_i}, \quad q \in \partial W_j, \quad i, j \in I_n, \quad (17)$$

using the boundary decomposition (15) and the fact that $\frac{\partial f(z_j)}{\partial z_i} = \frac{\partial f(z_i)}{\partial \theta_i} = \frac{\partial f(z_j)}{\partial \theta_i} = 0$ we obtain

$$\begin{aligned} \frac{\partial \mathcal{H}}{\partial z_i} &= \int_{W_i} f^d(z_i) \phi(q) dq + \int_{\partial W_i \cap \partial \mathcal{O}} v_i^i \cdot n_i f(z_i) \phi(q) dq + \\ &\sum_{j \in \mathcal{N}_i} \left[\int_{\partial W_i \cap \partial W_j} v_i^i \cdot n_i (f(z_i) - f(z_j)) \phi(q) dq \right] \end{aligned}$$

and

$$\begin{aligned} \frac{\partial \mathcal{H}}{\partial \theta_i} &= \int_{\partial W_i \cap \partial \mathcal{O}} \tau_i^i \cdot n_i f(z_i) \phi(q) dq + \\ &\sum_{j \in \mathcal{N}_i} \left[\int_{\partial W_i \cap \partial W_j} \tau_i^i \cdot n_i (f(z_i) - f(z_j)) \phi(q) dq \right] \end{aligned}$$

VI. SIMULATION STUDIES

Simulation studies used to evaluate the efficiency of the proposed control scheme are presented in this section. The region of interest Ω is chosen to be the same as in [4] for consistency. All nodes are identical with an elliptical base sensing pattern and altitude constraints $z^{\min} = 0.3$ and $z^{\max} = 2.3$. The nodes' initial states, excluding their altitude, are the same as in [11]. The boundaries of the nodes' cells are shown in solid black and the boundaries of their sensing regions in dashed red lines. It should be noted that although for some sensing patterns, such as circular ones, it is possible to derive the stable altitude for a single MAA, this is not the case with elliptical sensing patterns. This is due to the fact that there exists no closed-form expression for the arc length of an ellipse. The simulations used in this section have been implemented in Matlab and are available as free and open-source software in <https://git.sr.ht/~sotiris/p/uav-coverage>. The code is written from the scope of a single agent, thus it can be easily modified and used as a basis for a real world implementation.

A. Case Study I

In this simulation study the elliptical sensing patterns are approximated by their largest inscribed disks centered at q_i with radii r_b^{\min} . In that case, only control laws (11) and (12) are used, since the sensing patterns are rotation invariant. The resulting control scheme is the one examined in [24]. Figure 8 (top) shows the evolution of the network through time, with the real elliptical sensing patterns shown by dotted black lines. The coverage quality at the initial and final configurations of the network are shown in Figure 5 while the value of the optimization criterion and the percentage of covered area are shown in Figure 9 in blue.

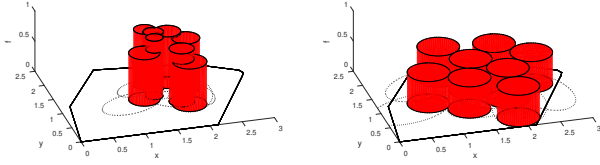


Fig. 5. Case Study I: Initial [Left] and final coverage quality.

B. Case Study II

In this simulation study the exact elliptical sensing patterns of the nodes are used, however their orientations remain fixed to their initial values. Thus, again only control laws (11) and (12) are used. Figure 8 (middle) shows the evolution of the network through time while the coverage quality at the initial and final configurations of the network are shown in Figure 6. The value of the optimization criterion and the percentage of covered area are shown in Figure 9 in red.

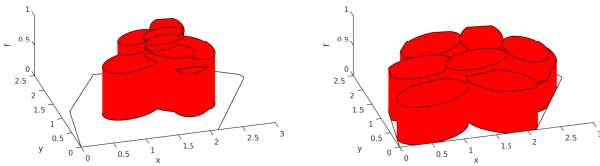


Fig. 6. Case Study II: Initial [Left] and final coverage quality.

C. Case Study III

In this final simulation study the complete control scheme (11), (12) and (13) is used in conjunction with the elliptical sensing patterns. Figure 8 (middle) shows the evolution of the network through time while the coverage quality at the initial and final configurations of the network are shown in Figure 7. The value of the optimization criterion and the percentage of covered area are shown in Figure 9 in green.

It is clear from Figure 9 that a maximal inscribed circle approximation of the sensed region can severely limit the efficiency of the agents. Even when the agents are not allowed to rotate, the network's performance is significantly improved when the exact sensing patterns are used compared to their circular approximations. However, in such a case the agents are not always used to their full potential, as can be seen in Figure 8 (middle) [Right] where the sensing region of an agent is completely contained within that of another.

VII. CONCLUSIONS

Area coverage by a network of MAAs has been examined in this article. Each MAA is equipped with a downwards facing camera with a generic convex sensing pattern. A partitioning of the region sensed by all MAAs is used to assign regions of responsibility to each one of them and based on them a gradient-based control law is derived. The

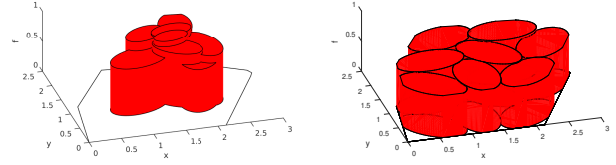


Fig. 7. Case Study III: Initial [Left] and final coverage quality.

control law maximizes a combined coverage-quality optimization criterion. Simulation studies were provided in order to evaluate the proposed control scheme and compare its performance with that of other simplified control strategies for the same problem.

REFERENCES

- [1] J. Cortés, S. Martinez, and F. Bullo, "Spatially-distributed coverage optimization and control with limited-range interactions," *ESAIM: Control, Optimisation and Calculus of Variations*, vol. 11, no. 4, pp. 691–719, October 2005.
- [2] L. Pimenta, V. Kumar, R. Mesquita, and G. Pereira, "Sensing and coverage for a network of heterogeneous robots," in *47th IEEE Conference on Decision and Control (CDC)*, Cancun, Mexico, December 2008, pp. 3947–3952.
- [3] J. Cortés, S. Martinez, T. Karatas, and F. Bullo, "Coverage control for mobile sensing networks," *IEEE Transactions on Robotics and Automation*, vol. 20, no. 2, pp. 243–255, April 2004.
- [4] Y. Stergiopoulos and A. Tzes, "Convex Voronoi-inspired space partitioning for heterogeneous networks: A coverage-oriented approach," *IET Control Theory & Applications*, vol. 4, no. 12, pp. 2802–2812, December 2010.
- [5] O. Arslan and D. E. Koditschek, "Voronoi-based coverage control of heterogeneous disk-shaped robots," in *IEEE International Conference on Robotics and Automation (ICRA)*, May 2016, pp. 4259–4266.
- [6] F. Mohseni, A. Doustmohammadi, and M. B. Menhaj, "Distributed receding horizon coverage control for multiple mobile robots," *IEEE Systems Journal*, vol. 10, no. 1, pp. 198–207, June 2014.
- [7] V. Ramaswamy and J. R. Marden, "A sensor coverage game with improved efficiency guarantees," in *American Control Conference (ACC)*, Boston, MA, USA, July 2016, pp. 6399–6404.
- [8] Y. Stergiopoulos and A. Tzes, "Spatially distributed area coverage optimisation in mobile robotic networks with arbitrary convex anisotropic patterns," *Automatica*, vol. 49, no. 1, pp. 232–237, January 2013.
- [9] Y. Kantaros, M. Thanou, and A. Tzes, "Distributed coverage control for concave areas by a heterogeneous robot-swarm with visibility sensing constraints," *Automatica*, vol. 53, pp. 195–207, March 2015.
- [10] D. Panagou, D. M. Stipanović, and P. G. Voulgaris, "Distributed dynamic coverage and avoidance control under anisotropic sensing," *IEEE Transactions on Control of Network Systems*, vol. 4, no. 4, pp. 850–862, June 2016.
- [11] Y. Stergiopoulos and A. Tzes, "Cooperative positioning/orientation control of mobile heterogeneous anisotropic sensor networks for area coverage," in *IEEE International Conference on Robotics and Automation (ICRA)*, Hong Kong, China, May 2014, pp. 1106–1111.
- [12] E. Bakolas, "Distributed partitioning algorithms for multi-agent networks with quadratic proximity metrics and sensing constraints," *Systems & Control Letters*, vol. 91, pp. 36–42, May 2016.
- [13] Y. Stergiopoulos, M. Thanou, and A. Tzes, "Distributed collaborative coverage-control schemes for non-convex domains," *IEEE Transactions on Automatic Control*, vol. 60, no. 9, pp. 2422–2427, March 2015.
- [14] R. J. Alitappeh, K. Jeddisaravi, and F. G. Guimarães, "Multi-objective multi-robot deployment in a dynamic environment," *Soft Computing*, vol. 21, pp. 6481–6497, June 2016.
- [15] A. Renzaglia, L. Doitsidis, E. Martinelli, and E. Kosmatopoulos, "Multi-robot three-dimensional coverage of unknown areas," *The International Journal of Robotics Research*, vol. 31, no. 6, pp. 738–752, May 2012.

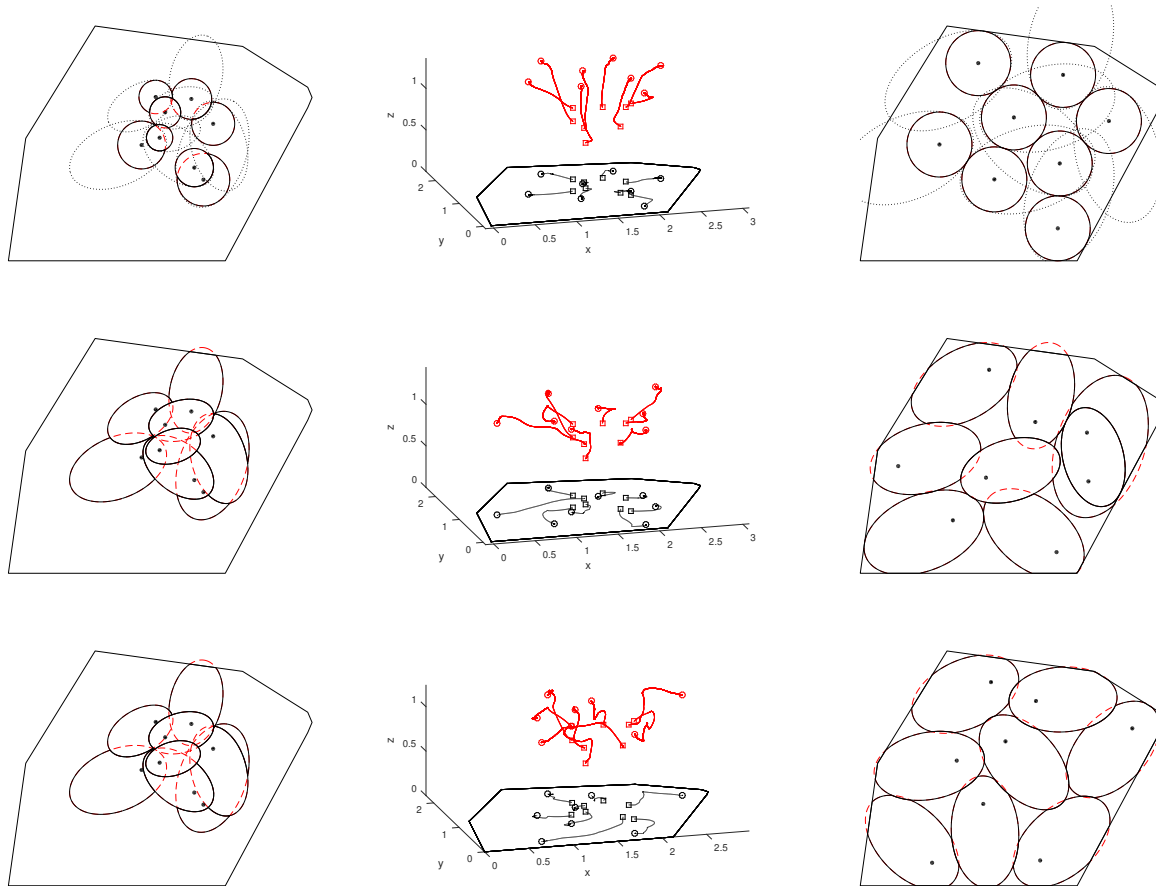


Fig. 8. Initial network state [Left], agent trajectories [Center] and final network state [Right] for Case Study I (top), Case Study II (middle) and Case Study III (bottom).

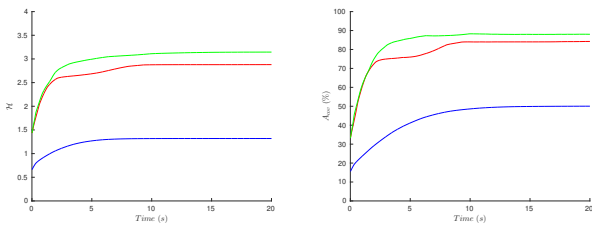


Fig. 9. Coverage-quality objective \mathcal{H} [Left] and percentage of Ω covered [Right].

- [16] A. Breitenmoser, J. Metzger, R. Siegwart, and D. Rus, "Distributed coverage control on surfaces in 3D space," in *IEEE/RSJ International Conference on Intelligent Robots and Systems*, Taipei, Taiwan, December 2010, pp. 5569–5576.
- [17] M. Thanou and A. Tzes, "Distributed visibility-based coverage using a swarm of UAVs in known 3D-terrains," in *6th International Symposium on Communications, Control and Signal Processing (ISCCSP)*, Athens, Greece, May 2014, pp. 425–428.
- [18] M. Torres, D. A. Pelta, J. L. Verdegay, and J. C. Torres, "Coverage path planning with unmanned aerial vehicles for 3D terrain reconstruction," *Expert Systems with Applications*, vol. 55, pp. 441–451, 2016.
- [19] M. Schwager, B. J. Julian, and D. Rus, "Optimal coverage for multiple hovering robots with downward facing cameras," in *IEEE International Conference on Robotics and Automation (ICRA)*, Kobe, Japan, May 2009, pp. 3515–3522.

- [20] M. Schwager, B. J. Julian, M. Angermann, and D. Rus, "Eyes in the sky: Decentralized control for the deployment of robotic camera networks," *Proceedings of the IEEE*, vol. 99, no. 9, pp. 1541–1561, July 2011.
- [21] J. Hu, L. Xie, and J. Xu, "Vision-based multi-agent cooperative target search," in *12th International Conference on Control Automation Robotics & Vision (ICARCV)*, Guangzhou, China, December 2012, pp. 895–900.
- [22] E. Yanmaz, "Connectivity versus area coverage in unmanned aerial vehicle networks," in *IEEE International Conference on Communications (ICC)*, Ottawa, ON, Canada, June 2012, pp. 719–723.
- [23] M. A. Messous, S. M. Senouci, and H. Sedjelmaci, "Network connectivity and area coverage for UAV fleet mobility model with energy constraint," in *IEEE Wireless Communications and Networking Conference*, Doha, Qatar, April 2016, pp. 1–6.
- [24] S. Papatheodorou, A. Tzes, and Y. Stergiopoulos, "Collaborative visual area coverage," *Robotics and Autonomous Systems*, vol. 92, pp. 126–138, June 2017.
- [25] K. Alexis, G. Nikolakopoulos, and A. Tzes, "Switching model predictive attitude control for a quadrotor helicopter subject to atmospheric disturbances," *Control Engineering Practice*, vol. 19, no. 10, pp. 1195–1207, October 2011.
- [26] C. Di Franco and G. Buttazzo, "Coverage path planning for UAVs photogrammetry with energy and resolution constraints," *Journal of Intelligent & Robotic Systems*, vol. 83, pp. 445–462, February 2016.
- [27] G. S. Avellar, G. A. Pereira, L. C. Pimenta, and P. Iscold, "Multi-UAV routing for area coverage and remote sensing with minimum time," *Sensors*, vol. 15, no. 11, pp. 27 783–27 803, November 2015.